Clinical and Experimental Medicine (2025) 25:170
https://doi.org/10.1007/s10238-025-01556-8

RESEARCH

Identification and validation a novel kinase-related gene signature for predicting prognosis and responsiveness to immunotherapy in hepatocellular carcinoma

Yaju Qiu[1] · Xitian Wu[2] · Yang Luo[2] · Lianqiang Shen[3] · Anyang Guo[2] · Jing Jiang[2] · Lijuan Zhu[2] · Yuhua Zhang[2] · Fang Han[2] · Enyan Yu[4]

Received: 17 October 2024 / Accepted: 2 January 2025
© The Author(s) 2025

Abstract

Liver cancer research highlights the kinome's critical role in disease initiation and progression. However, comprehensive data analysis on the kinome's impact on hepatocellular carcinoma (HCC) prognosis is limited. We used the TCGA-LIHC mRNA expression profiles, analyzing them with various R packages. Key methods included univariate Cox regression for prognostic gene identification, consensus clustering for subtype classification, Gene Set Enrichment Analysis (GSEA), and immune landscape evaluation. A prognostic model was developed using LASSO Cox regression, and chemotherapy drug sensitivity was assessed using the pRRophetic package. We identified 45 kinases-related differentially expressed genes (DEGs), with 27 linked to HCC prognosis. Cluster analysis divided these genes into two subtypes, with distinct prognoses. We discovered 157 DEGs between kinase-related subtypes, 120 of which were prognostically relevant. A kinase-related gene signature (KRS) was developed for prognostic prediction. The high-KRS group showed poorer survival in TCGA-LIHC and validation cohorts, with notable differences in immune cell infiltration and checkpoint gene expression. This group also showed varying sensitivity to common drugs and anti-PD-L1 treatment. In contrast, the low-KRS group might respond better to anti-PD-1 immunotherapy. Our study introduces a kinase-related gene signature as a novel tool for predicting HCC prognosis. This signature aids in tailoring personalized treatment strategies, potentially improving clinical outcomes in HCC patients.

Keywords Hepatocellular carcinoma · Kinase · Tumor immune microenvironment · Prognosis · Immunotherapy

Introduction

Based on GLOBOCAN data, liver cancer stands as the seventh most prevalent cancer globally, with hepatocellular carcinoma (HCC) constituting 90% of cases, and it ranks fourth among the leading causes of cancer-related fatalities [1–3]. The incidence of new cases amounted to 905,677, representing 4.7% of all cancer cases, and liver cancer claimed 830,180 lives, accounting for 8.3% of global cancer-related deaths [2]. Noteworthy strides have been made in the clinical treatment of liver cancer in recent decades, encompassing modalities such as surgery, radiotherapy, targeted therapy, systemic therapy, and liver transplantation [4]. Despite the availability of promising treatment modalities, the prognosis for HCC remains bleak, primarily due to heightened risks of recurrence and metastasis. Advanced HCC, in particular, exhibits a 5-year survival rate not exceeding 12% [5]. Furthermore, individuals with HCC sharing comparable clinicopathological characteristics and tumor stages may encounter

Yaju Qiu, Xitian Wu and Yang Luo have Contributed equally.

✉ Fang Han
exodusf@163.com

✉ Enyan Yu
yuenyan@aliyun.com

[1] The Second School of Clinical Medicine, Zhejiang Chinese Medical University, Hangzhou 310053, Zhejiang, China

[2] Hepatobiliary and Pancreatic Surgery Department, The Zhejiang Cancer Hospital, Hangzhou 310022, Zhejiang, China

[3] Department of General Surgery, The First People's Hospital of Linping District, Hangzhou 311100, Zhejiang, China

[4] Department of Clinical Psychology, Zhejiang Cancer Hospital, Hangzhou 310012, Zhejiang, China

Published online: 20 May 2025

disparate prognoses attributable to individual variabilities [6, 7]. Consequently, the identification of potential prognostic factors assumes paramount importance in augmenting the overall outlook for patients grappling with HCC.

Kinases, a broad class of enzymes, play a key role in the process of phosphorylation, wherein they facilitate the transfer of high-energy phosphate groups from donor molecules, such as ATP, to specific target molecules [8]. These enzymes constitute about 2% of the human genome, forming an extensive array known as the human kinome, which includes 538 kinases. These kinases are instrumental in catalyzing protein phosphorylation [9]. Distributed across various cellular compartments, including the nucleus, mitochondria, microsomes, and cytoplasm [10], protein kinases are known to covalently attach to the hydroxyl groups of serine, threonine, or tyrosine residues on specific protein substrates. This action alters the conformation and activity of proteins and enzymes, playing a significant role in modulating biological processes [11]. Protein kinases are systematically classified into groups, families, and subfamilies, reflecting the complexity and diversity of their functions [12]. They are integral to a variety of cellular processes, including immunity, cell growth and division, and metabolism, highlighting their essential role in cellular signal transduction [13, 14]. In addition to protein kinases, there exists a class of kinases that target small molecules such as lipids, sugars, amino acids, and nucleosides. These kinases are crucial for initiating signaling cascades and preparing substrates for a range of metabolic reactions [15].

Protein kinases are central to the regulation of nearly all cellular functions, as evidenced by extensive research [13, 16, 17]. Dysregulation in kinase signaling, manifested through various abnormalities such as overexpression, aberrant localization, point mutations, or disruptions in upstream signaling pathways, has been implicated in the development of cancer and a range of human disorders [12, 18–20]. The intricate and multifaceted roles of kinases in cellular processes make them promising targets for therapeutic interventions in various diseases [21]. To date, the US Food and Drug Administration (FDA) has approved a broad spectrum of small molecule inhibitors designed to target specific kinases [12, 22]. Advancements in the understanding of kinase functions are not only pivotal in elucidating cancer biology but also instrumental in the rapid identification of potential agonists and antagonists for these enzymes. Such progress is crucial in fostering the development of targeted therapies for a wide array of diseases.

Initial investigations have underscored the pivotal association between the kinome and the initiation and progression of liver cancer. Earlier studies have concentrated on the capacity of kinases to provoke senescence in liver cancer cells[23]. Currently, the multi-kinase inhibitors sorafenib and lenvatinib have emerged as the first-line treatment drugs for liver cancer[24]. While extensive data mining studies have been conducted in various cancer types, research specifically examining the impact of the kinome on the progression and prognosis of hepatocellular carcinoma (HCC) remains limited. To address this gap, our investigation involved a comprehensive analysis of kinase transcriptome data obtained from publicly accessible databases containing liver cancer samples. From this analysis, we developed a prognostic multigene signature, consisting of eight kinase-related genes, aimed at accurately assessing the prognostic risk in HCC patients. To further explore the significance of this gene signature, we conducted a detailed assessment to determine its association with several key aspects. These include tumor immune cell infiltration, the tumor immune microenvironment, response to immunotherapy, and drug sensitivity in HCC.

Material and methods

Data collection

In this study, we accessed transcriptomic data for hepatocellular carcinoma (HCC) samples from The Cancer Genome Atlas (TCGA) database (https://portal.gdc.cancer.gov/). This dataset comprised 50 normal and 371 liver cancer samples. We also obtained associated clinical information for these patients from the UCSC Xena database (https://xenabrowser.net/heatmap/). After excluding samples without survival data, a total of 365 tumor samples were retained for cluster analysis. In addition, we utilized data from the International Cancer Genome Consortium (ICGC) database (https://icgc.org/), which provided a validation cohort comprising 231 HCC samples, hereinafter referred to as the ICGC cohort. Our analysis incorporated a list of 538 kinase-related genes, as identified in prior research [25] and detailed in Supplementary Table 1. To further support our findings, we gathered data from 258 HCC patients at Zhejiang Cancer Hospital to validate the identified hub genes.

Differentiated gene screening and enrichment analysis

For the differential expression analysis of kinome-associated genes, we employed the Limma package in R [26]. A stringent criterion was applied, using a false discovery rate (FDR) of 0.05 and a log fold change (logFC) threshold of 1. To better understand the biological characteristics of the differentially expressed genes (DEGs), we conducted enrichment analysis via the Metascape online database (https://metascape.org/gp/index.html) [27]. This platform was instrumental in identifying protein–protein interaction (PPI) networks and MCODE components within our gene

lists. Furthermore, we utilized the Sangerbox online analysis tool (http://vip.sangerbox.com/home.html) to investigate potential somatic mutations in HCC patients.

Consensus clustering

To identify prognostic kinase-related genes, univariate Cox regression analysis ($p < 0.05$) was executed utilizing the "survival" package in R. Subsequently, we applied unsupervised consensus clustering to these genes based on their expression profiles, employing the "ConsensusClusterPlus" package in R [28]. Kaplan–Meier survival curves were generated to compare overall survival (OS) across the different clusters. Additionally, Principal Component Analysis (PCA) was conducted using the "stats" package to validate the clustering results.

Development and validation of a gene signature associated with kinase-related genes

For the creation of a kinase-associated gene signature, DEGs among clusters were pinpointed using the "limma" package in R. The criteria set for this included a threshold of $|\log FC| < 1$ and an FDR < 0.05. Prognostic DEGs identified through univariable Cox regression analysis ($p < 0.05$) were then subjected to LASSO Cox regression analysis using the "glmnet" package. This process culminated in a gene model that calculates the Kinase-Related Score (KRS) for each HCC sample in the TCGA-LIHC cohort. The KRS formula is defined as $KRS = \Sigma(Coef\_i \times Exp\_i)$, where Coef_i represents the beta coefficient of gene i, and Exp_i indicates its expression level. Patients were divided into high- and low-KRS groups based on the median score, and the OS and predictive accuracy of the KRS were assessed via Kaplan–Meier analysis and time-dependent ROC curves, using the "survival" and "timeROC" packages, respectively. Furthermore, the KRS was validated with liver cancer samples from the ICGC cohort. Both univariate and multivariate Cox regression analyses were conducted in the TCGA-LIHC and validation cohorts to establish the independent prognostic value of the KRS.

Assessment of the immune landscape

To evaluate the abundance of immune infiltrating cells in each hepatocellular carcinoma (HCC) patient from the TCGA database, we employed single-sample gene set enrichment analysis (ssGSEA) and CIBERSORT algorithms [29]. The 'estimate' R package was utilized to calculate immune and stromal scores for each HCC sample [30]. A range of algorithms, including XCELL, TIMER, QUANTISEQ, MCPCOUNTER, EPIC, CIBERSORT-ABS, and CIBERSORT, were used to assess the infiltration levels of different immune cells in these samples [31]. Additionally, microsatellite instability (MSI) scores for each patient were obtained using the Sangerbox online tool (version 3.0).

Functional enrichment analysis

Gene Set Enrichment Analysis (GSEA) was conducted to explore the biological differences among various groups, utilizing gene expression data from the TCGA-LIHC cohort. This analysis was performed with the Sangerbox tool (version 3.0), referencing the h.all.v7.4.symbols.gmt gene set [32]. Pathways with a p-value below 0.05 were deemed statistically significant. Furthermore, the ClusterProfiler, org.Hs.eg.db, and ggplot2 packages in R were used for enrichment analysis of Gene Ontology (GO) and Kyoto Encyclopedia of Genes and Genomes (KEGG) databases to elucidate key biological characteristics of these genes [33].

Development and verification of nomogram

A nomogram was developed to predict the prognosis of HCC patients in the TCGA-LIHC cohort, integrating the prognostic gene signature and pertinent clinicopathological parameters, using the 'rms' R package. The accuracy of this nomogram in predicting actual survival outcomes was evaluated through calibration curves. Its clinical utility was further assessed via decision curve analysis (DCA) and receiver operating characteristic (ROC) curves, utilizing the “rms”, “rmda”, and “timeROC” R packages.

Drug sensitivity prediction

In this research, we examined two patient cohorts undergoing immunotherapy to assess their response in relation to the KRS. The first cohort, named IMvigor210, included patients with advanced urothelial cancer undergoing treatment with atezolizumab, an anti-PD-L1 antibody. The relevant data for this cohort were accessed from http://research-pub.Gene.com/imvigor210corebiologies. The second cohort, GSE78220, comprised patients with melanoma treated with pembrolizumab, an anti-PD-1 antibody. Data for this cohort were sourced from https://www.ncbi.nlm.nih.gov/geo/query/acc.cgi?acc=GSE78220. Additionally, to predict chemotherapy sensitivity in HCC patients, we utilized the 'pRRophetic' R package. This package estimates the half-maximum inhibitory concentration (IC50) of various chemotherapy drugs based on data from the Genomics of Drug Sensitivity in Cancer (GDSC) database [34, 35] (https://www.cancerrxgene.org/).

Tissue specimen collection and qRT-PCR analysis

Paired cancerous and normal tissues were collected from 20 HCC patients at Zhejiang Cancer Hospital. RNA was isolated from these tissues using the RNA Easy Fast Tissue Kit (Tiangen, China) and converted into cDNA using a reverse transcription kit (Monad, China). Quantitative real-time PCR (qRT-PCR) was performed with ChamQ Universal SYBR qPCR Master Mix (Vazyme, China) to determine gene expression levels. The $2-\Delta\Delta Ct$ method was applied for relative quantification. Primer sequences are provided in Supplementary Table 2.

Statistical analysis

For the analysis of categorical data, the chi-square test was applied. Continuous variables were evaluated using either the Mann–Whitney test or the Kruskal–Wallis test, dependent on the distribution of the data. All statistical tests were conducted as two-sided, with a P-value threshold of less than 0.05 set for indicating statistical significance. These analyses were carried out using R software (version 4.1.0).

Results

The expression and variation of kinase-related genes in HCC samples

This study aimed to explore the variation patterns of genes related to kinases in patients with HCC using the TCGA-LIHC cohort (Fig. 1). Out of 538 kinase-related genes, we found that 45 were expressed differentially between HCC and normal tissues. Specifically, the expression levels of 42 genes were upregulated in cancerous tissues, while 3 genes were downregulated, with all DEGs listed in Supplementary Table 3. Figure 2A shows a heatmap of the key kinase-related genes, while Fig. 2B displays a volcano plot. The results of the enrichment analysis revealed that the identified key genes exhibited significant enrichment in diverse biological functions associated with protein phosphorylation. These functions encompassed a spectrum of processes, notably protein phosphorylation, peptidyl-serine phosphorylation, protein autophosphorylation, and peptidyl-tyrosine phosphorylation. Furthermore, the

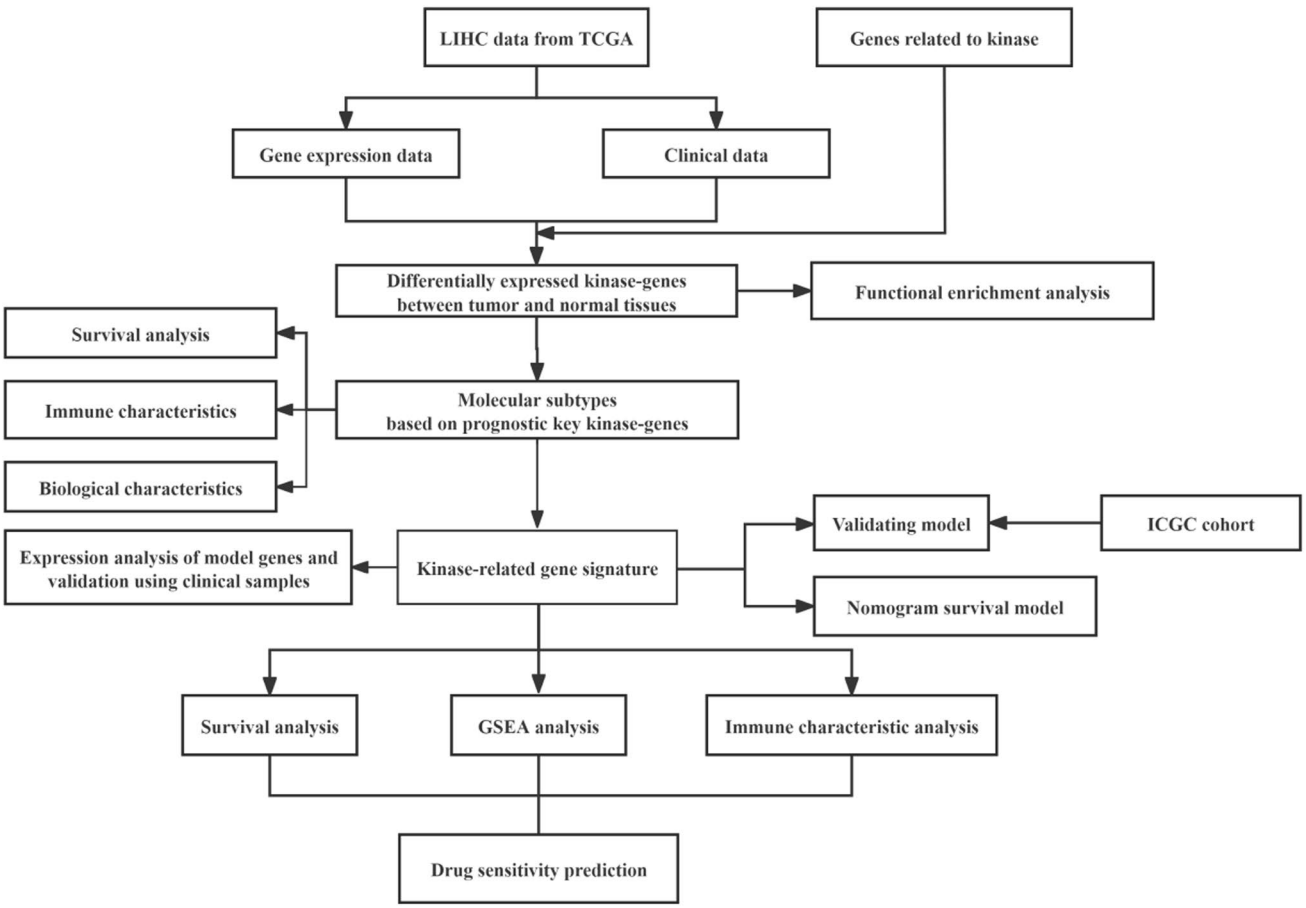

Fig. 1 A flow diagram of the research design

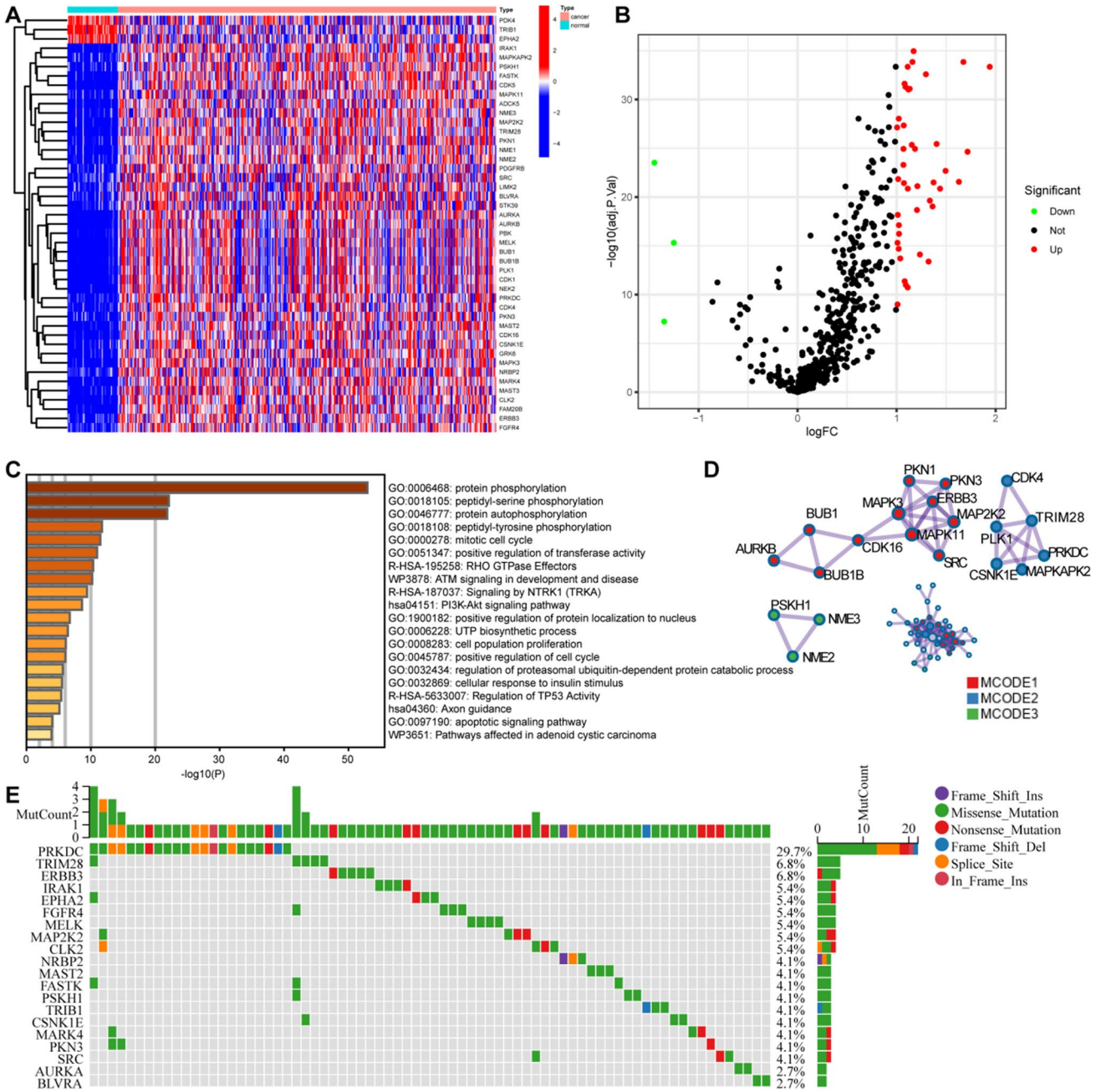

Fig. 2 The expression and variation of kinase-related genes in HCC patients. (**A**) Heatmap of the differentially expressed (DE) kinase-related genes between tumor and normal tissues. (**B**) Volcano plot of the DE-kinase-related genes in tumor and normal tissues (green: down-regulated DEGs; red: up-regulated DEGs; grey: unchanged genes). (**C**) Enrichment analyses based on the DE-kinase-related genes. (**D**) PPI network based on the DE-kinase-related genes. (**E**) An oncoplot of DE-kinase-related genes in the TCGA-LIHC cohort

enriched biological processes extended to cancer-related pathways, including the mitotic cell cycle, cell population proliferation, positive regulation of the cell cycle, PI3K-Akt signaling pathway, regulation of TP53 activity, and axon guidance (Fig. 2C). The protein–protein interaction network and MCODE components were identified in the key gene lists, as depicted in Fig. 2D. Furthermore, our study involved a thorough examination of genetic alterations in pivotal kinase-related genes among HCC patients from the TCGA cohort. This analysis resulted in the identification of the most prevalent mutations within the top 15 kinase-related genes. Remarkably, the PRKDC gene emerged as having the highest mutation frequency, recorded at 29.7%. In comparison, the mutation frequencies of the other genes in this group were found to range between 2.7 and 6.8%, as illustrated in Fig. 2E.

Identification of molecular subtypes based on prognostic key kinase-related genes

In this study, univariate Cox regression analysis was employed to pinpoint kinase-related genes with prognostic importance for HCC patients within the TCGA dataset. This analysis successfully identified 27 genes significantly correlated with survival ($P < 0.05$), as listed in Supplementary Table 4. Using these genes, we classified patients from the TCGA-LIHC cohort into two distinct clusters. These clusters demonstrated robust internal consistency and stability, as evidenced in Fig. 3A–C. PCA further highlighted a marked differentiation between the clusters (Fig. 3D). Notably, the expression levels of the majority of these 27 key prognostic kinase-related genes were elevated in cluster 2 relative to cluster 1, as shown in Fig. 3E. Survival analysis indicated that patients in cluster 2 had a significantly poorer prognosis compared to those in cluster 1 (Fig. 3F).

Immune characterization between different kinase-related subtypes

Cluster 1 and Cluster 2 displayed notable differences in various immune cell populations (Fig. 3G), encompassing B cells naive, B cells memory, T cells CD4 memory resting, T cells CD4 memory activated, T cells follicular helper, NK cells resting, macrophages M0/M2, and dendritic cells resting. Notably, Cluster 2 exhibited higher immune scores and lower stromal scores compared to Cluster 1 (Fig. 3H). Furthermore, an examination of the expression levels of six immune checkpoint genes, namely PDCD1, CD274, CTLA4, TIGIT, LAG3, and HAVCR2, revealed elevated expression in Cluster 2 relative to Cluster 1 (Fig. 3I).

Biological characteristics of kinase-related subtypes

To investigate the potential reasons for the different prognosis and immune characteristics observed between the two clusters, we examined the hallmark pathways enriched in each cluster. Using GSEA analysis, we found that cluster 1 was enriched in BILE_ACID_METABOLISM, XENOBIOTIC_METABOLISM, and FATTY_ACID_METABOLISM pathways (Fig. 4A). Additionally, cluster 1 exhibited upregulated expression of genes involved in DNA replication and cell cycle-related pathways, including E2F targets, G2M checkpoint, MYC targets, MTORC1, and PI3K-Akt pathway (Fig. 4A). In contrast, cluster 2 showed enrichment in cancer-related pathways such as PI3K_AKT_MTOR_SIGNALING and WNT_BETA_CATENIN_SIGNALING, as well as cell cycle-associated G2M_CHECKPOINT and E2F_TARGETS pathways (Fig. 4B). Furthermore, we identified 157 genes with differential expression levels between the two clusters (Supplementary Table 5), which were enriched in many biological functions and pathways, including cell cycle, Chemical carcinogenesis, p53 signaling pathway, Drug metabolism, and kinase activity (Fig. 4C, D).

Establishment and verification of a kinase-related gene signature in HCC

Establishment of kinase-related gene signature

In the initial phase of our analysis, we discerned 120 DEGs out of a total of 157, demonstrating a significant correlation with OS in HCC, as detailed in Supplementary Table 6. Subsequently, we employed LASSO Cox regression analysis to derive an 8-gene signature comprising UAP1L1, CENPA, TRIP13, PLGLA, CDCA8, PKIB, KIF20A, and SLC16A3 from these prognostic-kinase-related DEGs. Among the eight signature genes, seven were significantly upregulated in tumor tissues compared to normal tissues in the TCGA liver cancer dataset, while PLGAL was downregulated (Fig. S1). To validate these findings, we collected 20 pairs of clinical HCC and adjacent normal tissue samples and performed PCR experiments, which yielded results consistent with the findings from the TCGA liver cancer dataset (Fig. S2).

The KRS for each HCC patient was calculated using the following formula: KRS = (UAP1L1 × 0.0259) + (CENPA × 0.0336) + (TRIP13 × 0.0585) + (PLGLA × −0.0164) + (CDCA8 × 0.1891) + (PKIB × 0.0027) + (KIF20A × 0.0419) + (SLC16A3 × 0.0658). Based on this formula, HCC patients were stratified into high- and low-KRS groups, with the median KRS value of 0.578 serving as the threshold for categorization.

Evaluation and validation of kinase-related gene signature

Figure 5A presents the relationship between KRS and survival duration for each patient within the TCGA-LIHC cohort. PCA successfully distinguished between the high- and low-KRS groups, as shown in Fig. 5B. Kaplan–Meier survival analysis further revealed that the high-KRS group had significantly inferior OS, DFI, and PFI in comparison to the low-KRS group (Fig. 5E–G). To assess the prognostic accuracy of KRS, we constructed a ROC curve, which yielded AUC values of 0.746, 0.715, and 0.691 for 1-year, 2-year, and 3-year survival, respectively (Fig. 5I). Additionally, the prognostic efficacy of KRS was corroborated in a separate cohort of 231 HCC samples from the ICGC database, utilizing the same prognostic model (Fig. 5C–D, H, J). Kaplan–Meier analysis of this ICGC validation cohort confirmed that the high-KRS group had a shorter OS compared to the low-KRS group (Fig. 5H). The AUC values for KRS in the ICGC cohort were 0.759, 0.734, and 0.747 for 1-year, 2-year, and 3-year survival, respectively (Fig. 5J).

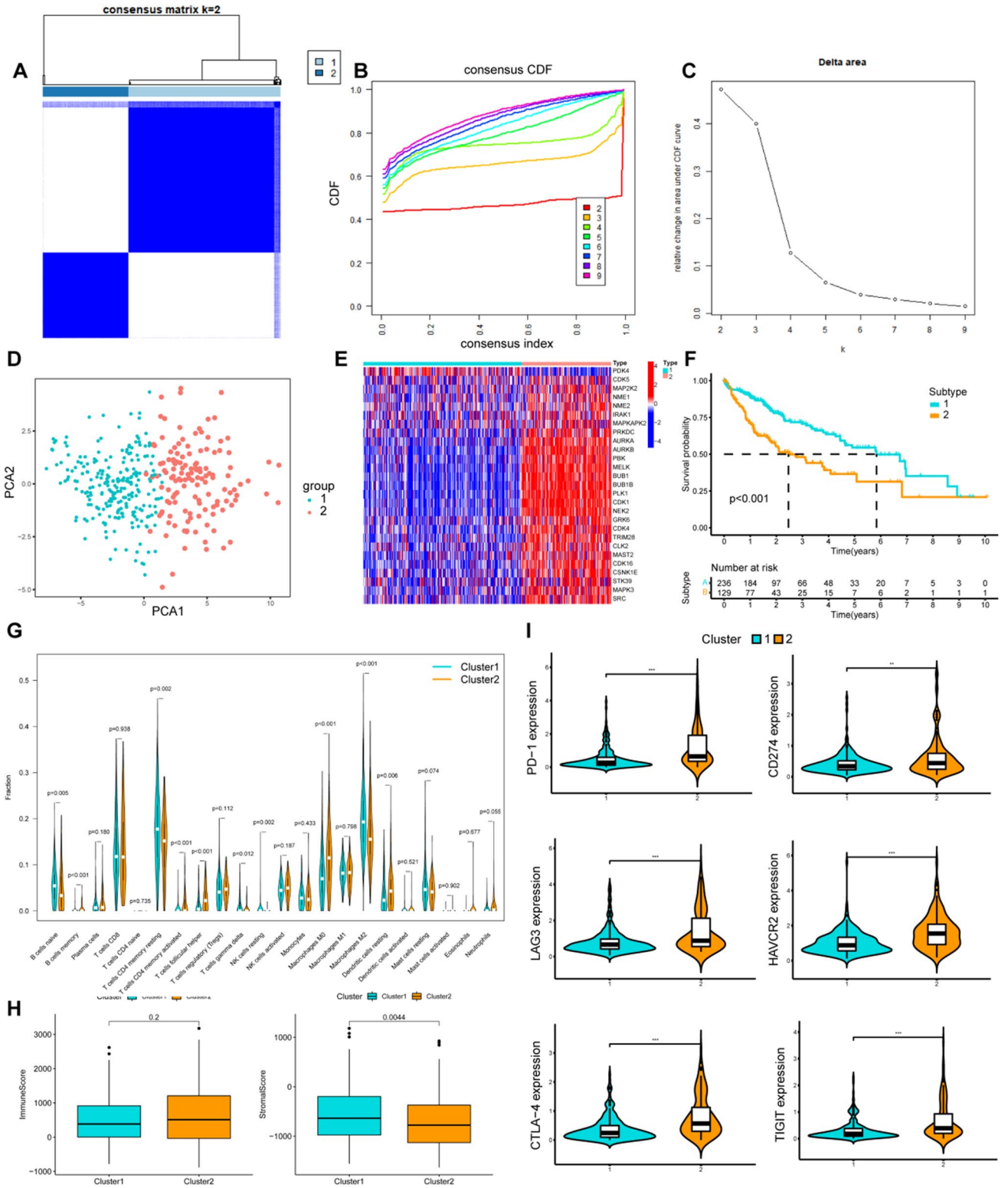

Fig. 3 Clinical and immune characteristics of kinase-related subtypes. (**A**) Consensus clustering matrix when k = 2. (**B**) Consensus clustering CDF with k valued 2–9. (**C**) Relative change in area under the CDF curve for k = 2 through 9. (**D**) PCA analysis showed that HCC could be well differentiated into two subtypes based on the expression of prognostic key kinase-related genes. (**E**) Heatmap of the 27 prognostic key kinase-related genes between cluster 1 and cluster 2. (**F**) Kaplan–Meier curves of OS for two subtypes in HCC. The expression of immune cell infiltration (**G**) and immune/stroma score (**H**) between different subtypes. (**I**) The expression levels of immune checkpoint genes between different subtypes. $*p < 0.05$, $**p < 0.01$, $***p < 0.001$

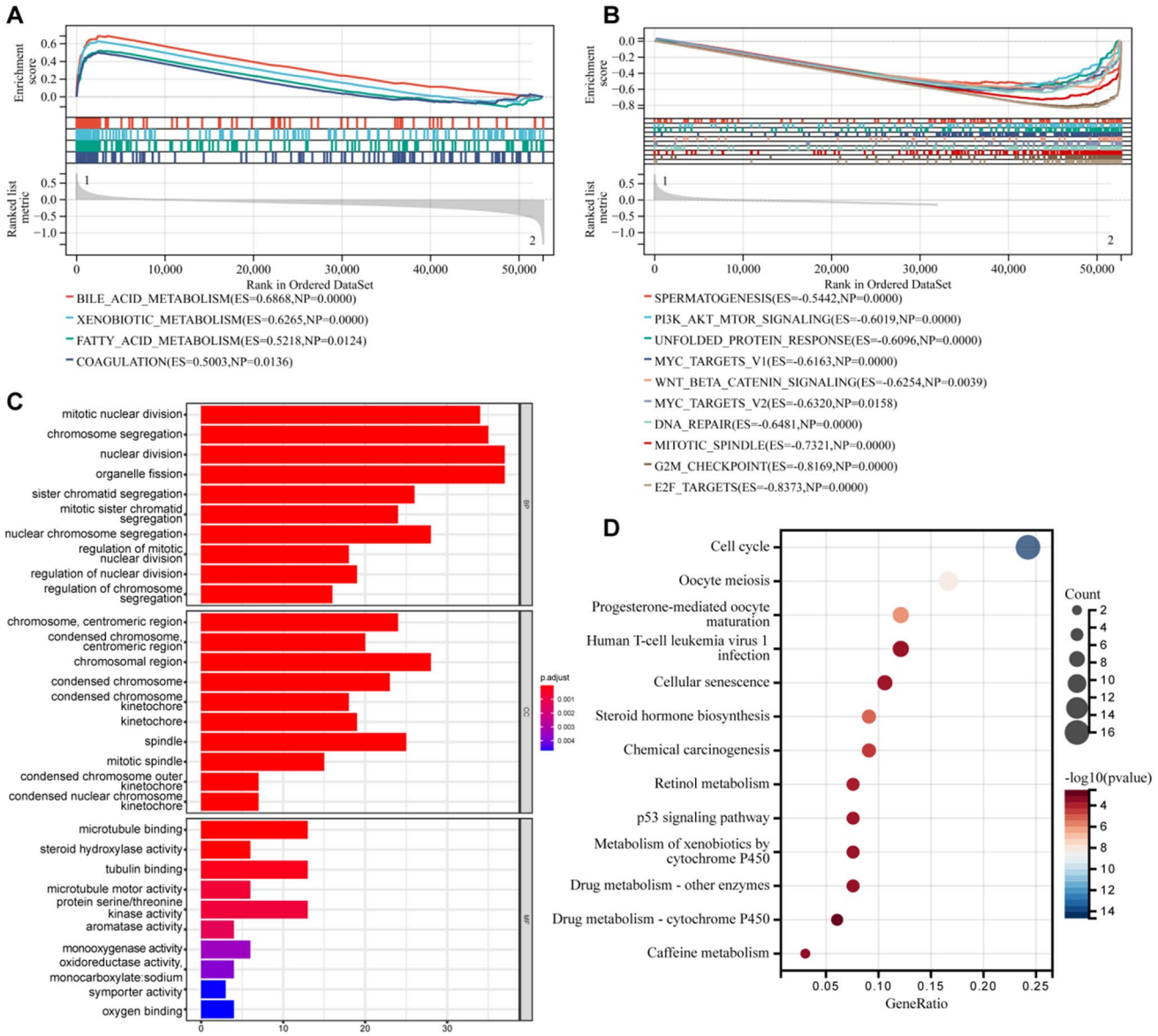

Fig. 4 Biological characterization of kinase-related subtypes. The GSEA pathway enrichment analysis in cluster 1 (**A**) and cluster 2 (**B**). (**C**) GO enrichment analyses based on the prognostic DEGs. adjusted $p < 0.05$. BP, biological process; CC, cellular component; MF, molecular function. (**D**) KEGG enrichment analyses based on the prognostic DEGs. $p < 0.05$

Collectively, these results highlight the effectiveness of our prognostic model, which is based on eight kinase-related genes, as a potent predictor of prognosis in HCC patients.

KRS is an independent prognostic predictor for HCC patients

The results from univariate Cox regression analysis in the TCGA cohort revealed statistically significant correlations between KRS, T-stage, M-stage, and pTNM staging, and OS, as illustrated in Fig. 6A. Subsequent multivariate Cox regression analysis identified KRS as an independent prognostic factor for OS, exhibiting a HR of 4.667 (95% CI: 2.461–8.853) with a *p*-value of less than 0.001 (Fig. 6B). Similar findings were replicated in the ICGC cohort, further substantiating KRS's role as an independent prognostic factor (Fig. 6C, D).

Development and validation of the nomogram prediction model

In addition to our analyses, we integrated the collected clinicopathological characteristics with the kinase-related gene signature to construct a prognostic nomogram. This tool

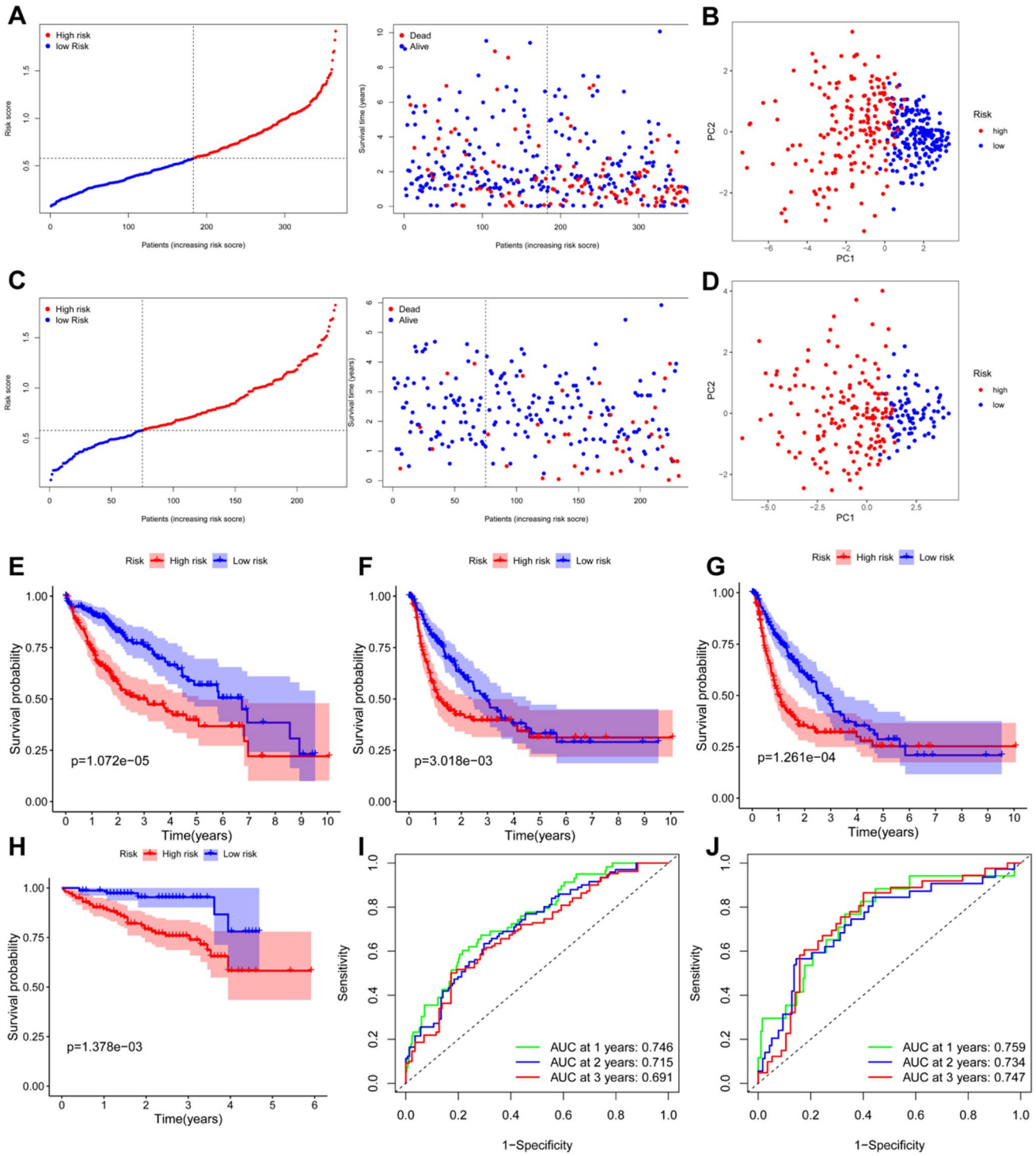

Fig. 5 Evaluation and validation of kinase-related gene signature. Distribution of KRS and survival time, PCA analysis in TCGA-LIHC (**A**, **B**) and ICGC (**C**, **D**) cohorts. Kaplan–Meier curves of OS (**E**), DFI (**F**) and PFI (**G**) in TCGA-LIHC cohort. Kaplan–Meier curves of OS in ICGC cohort (**H**). ROC curves of 1-, 2-, and 3-year OS in TCGA-LIHC (**I**) and ICGC cohorts (**J**)

is designed for accurately forecasting 1-year, 3-year, and 5-year OS rates of HCC patients within the TCGA-LIHC cohort, as depicted in Fig. 6E. To validate its predictive accuracy, calibration curves for these OS intervals were compared against the ideal reference line. The close alignment observed in these comparisons, illustrated in Fig. 6F, underscores the nomogram's robust predictive performance for the TCGA-LIHC cohort. Decision curve analysis (DCA)

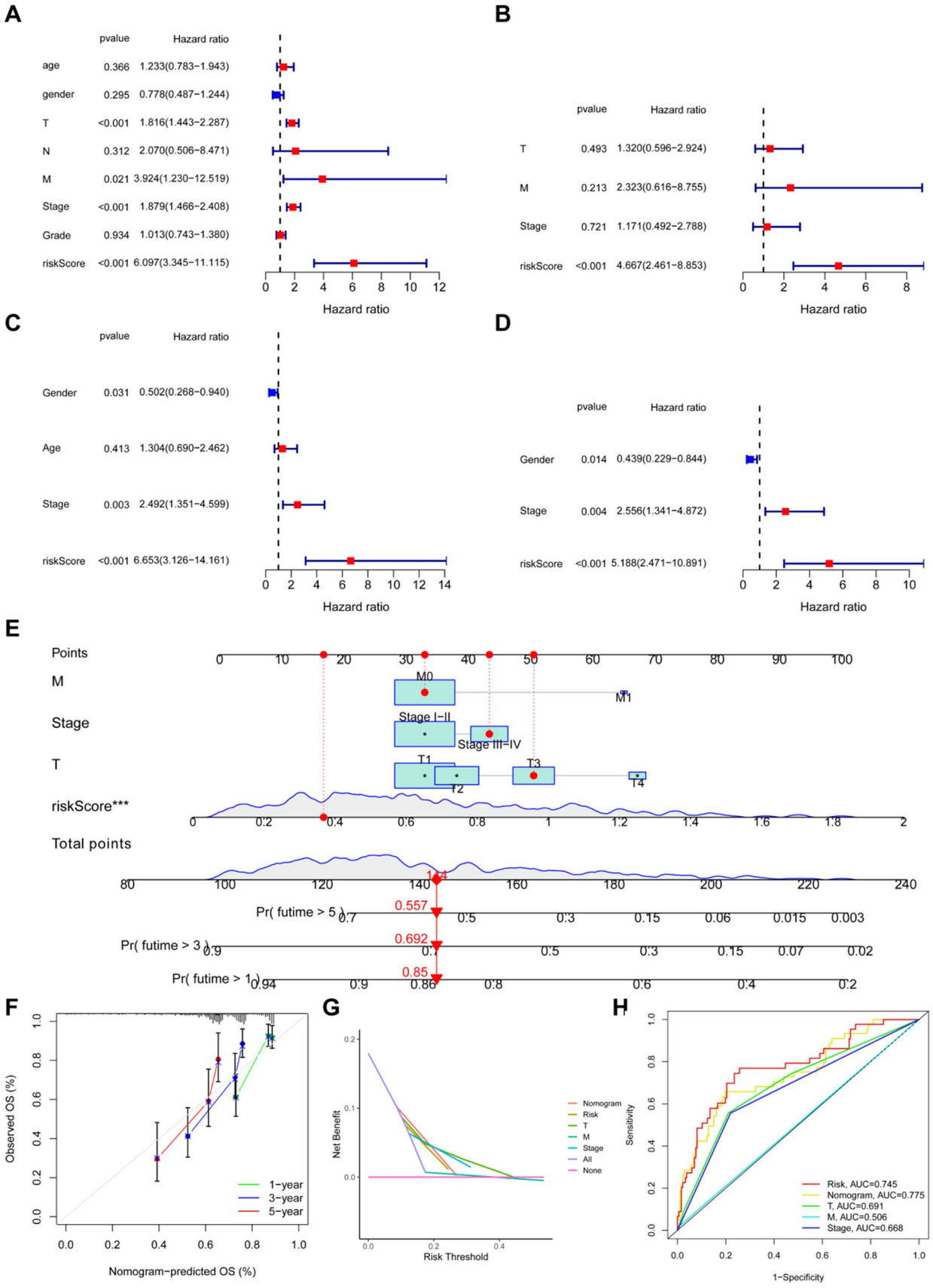
A
pvalue
Hazard ratio
age 0.366 1.233(0.783−1.943)
gender 0.295 0.778(0.487−1.244)
T <0.001 1.816(1.443−2.287)
N 0.312 2.070(0.506−8.471)
M 0.021 3.924(1.230−12.519)
Stage <0.001 1.879(1.466−2.408)
Grade 0.934 1.013(0.743−1.380)
riskScore <0.001 6.097(3.345−11.115)
Hazard ratio
B
pvalue
Hazard ratio
T 0.493 1.320(0.596−2.924)
M 0.213 2.323(0.616−8.755)
Stage 0.721 1.171(0.492−2.788)
riskScore <0.001 4.667(2.461−8.853)
Hazard ratio
C
pvalue
Hazard ratio
Gender 0.031 0.502(0.268−0.940)
Age 0.413 1.304(0.690−2.462)
Stage 0.003 2.492(1.351−4.599)
riskScore <0.001 6.653(3.126−14.161)
Hazard ratio
D
pvalue
Hazard ratio
Gender 0.014 0.439(0.229−0.844)
Stage 0.004 2.556(1.341−4.872)
riskScore <0.001 5.188(2.471−10.891)
Hazard ratio
E
Points
M
Stage
T
riskScore***
Total points
M0
M1
Stage I−II
Stage III−IV
T1
T2
T3
T4
Pr(futime > 5)
Pr(futime > 3)
Pr(futime > 1)
0.557
0.692
0.85
F
Observed OS (%)
Nomogram−predicted OS (%)
1−year
3−year
5−year
G
Net Benefit
Risk Threshold
Nomogram
Risk
T
M
Stage
All
None
H
Sensitivity
1−Specificity
Risk, AUC=0.745
Nomogram, AUC=0.775
T, AUC=0.691
M, AUC=0.506
Stage, AUC=0.668

◂**Fig. 6** Predictive nomogram. Univariate and multivariate analysis of the clinicopathologic features and the KRS in TCGA-LIHC (**A**, **B**) and ICGC (**C**, **D**) cohorts. (**E**) Nomogram to predict the survival of the HCC patients. (**F**) Calibration curve for 1-, 3-, and 5-year OS. DCA (**G**) and ROC (**H**) curve of the clinicopathologic features and KRS

further demonstrated the nomogram's superiority over other study predictors (Fig. 6G). The AUC values indicating high predictive accuracy for 5-year survival (Fig. 6H).

Biological features of low- and high-KRS groups

In our study, we delved into the underlying hallmark pathways that might account for the prognostic disparities observed between the low- and high-KRS groups in hepatocellular carcinoma. The analysis indicated a distinct enrichment of metabolism-related pathways in the low-KRS group, a finding that is clearly depicted in Fig. 7A. Conversely, the high-KRS group was characterized by a more pronounced involvement in cell cycle and cancer-related pathways, as detailed in Fig. 7B. This dichotomy in pathway activation underscores the potential mechanistic differences driving the varied prognoses associated with each KRS group.

KRS to assess tumor immune characteristic

To investigate the relationship between KRS and immune cell infiltration in HCC patients, we employed multiple analytical approaches to quantify the infiltration of diverse immune cells. This included conducting Spearman correlation analysis to elucidate the association between immune cell infiltration levels and KRS (Fig. 8A). Our analysis revealed a predominantly positive correlation between KRS and the infiltration of most immune cell types. This suggests that HCC patients with elevated KRS scores are likely to exhibit increased immune cell infiltration. Contrastingly, stroma scores demonstrated an inverse correlation with KRS. Utilizing the TIMER algorithm, we further delineated the disparities in immune cell infiltration between patients with high and low KRS scores. Notably, the high KRS group manifested significantly greater infiltration of B cells, neutrophils, macrophages, CD4+ T cells, and myeloid dendritic cells (Fig. 8B). Additionally, this group showed augmented expression levels of immune checkpoint genes (Fig. 8C), MSI scores (Fig. 8D), and MHC gene expression (Fig. 8E).

KRS to predict immunotherapy and chemotherapy responses

The analysis of the IMvigor210 cohort showed that patients with a higher KRS tended to respond better to anti-PD-L1 immunotherapy (Fig. 9A). On the other hand, in the GSE78220 cohort with anti-PD-1 immunotherapy, the low KRS group exhibited a significant clinical response compared to the high KRS group (Fig. 9B). We also evaluated the ability of the KRS to predict drug sensitivity for conventional chemotherapy drugs. Our findings revealed that the

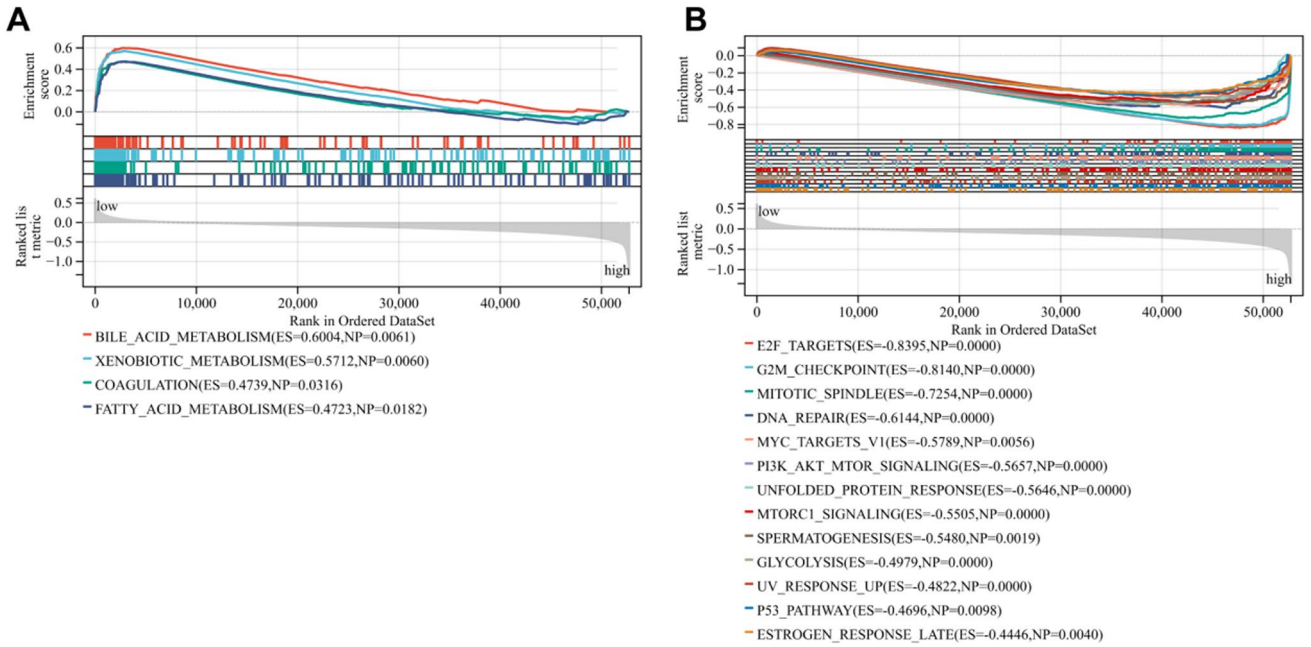

Fig. 7 Biological features of low- and high-KRS groups. The GSEA pathway enrichment analysis in low- (**A**) and high- (**B**) KRS groups

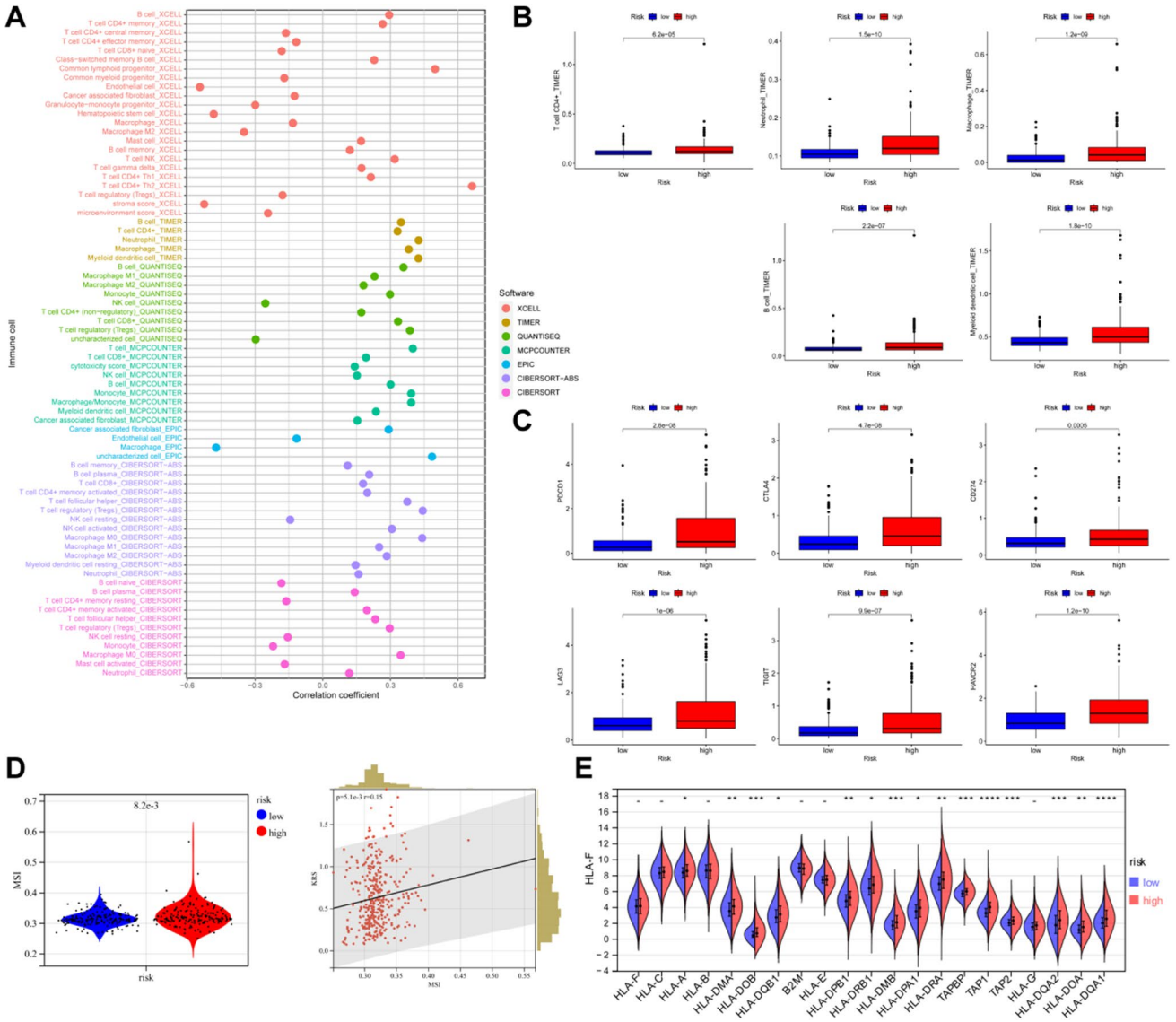

Fig. 8 KRS to assess tumor immune characteristic in HCC patients. The association between KRS and the multiple immune cell infiltration levels in TCGA-LIHC cohort (**A**). Boxplot for immune cell infiltration level (**B**) and immune checkpoint genes (**C**) between the high- and low-KRS groups. Violin and scatter plot for MSI scores between the high- and low- KRS groups (**D**). (**E**) Split violin plot for MHC genes between the high- and low-KRS groups

high KRS group had significantly lower IC50 values for all the tested drugs (Fig. 9C).

Kinase hub gene verification

To investigate the impact of genes associated with kinases on tumors, we performed tissue validation on the core genes within the aforementioned model. Firstly, subsequent to thorough analysis, we identified five genes (CDK4, PLK1, AURKA, AURKB, BUBIB) that hold significant prominence among the kinase-related genes (Fig. S3). We commenced by validating the differential expression of these five genes in tumors in comparison to the adjacent normal tissues. Our analysis revealed expression disparities in PLK1, AURKA, and AURKB, as illustrated in Fig. 10A. Moreover, we scrutinized the connection between these five genes and clinical phenotypes. Our analysis divulged that liver cirrhosis bears associations with AURKB, CDK4, and PLK1. Notably, AURKB experiences downregulation while CDK4 undergoes upregulation in instances of liver cirrhosis, as depicted in Fig. 10B. Additionally, regarding tumor necrosis, we observed elevated expressions of AURKB and PLK1 in the necrotic group, as opposed to the non-necrotic group, as illustrated in Fig. 10C. Finally, to gauge the potential

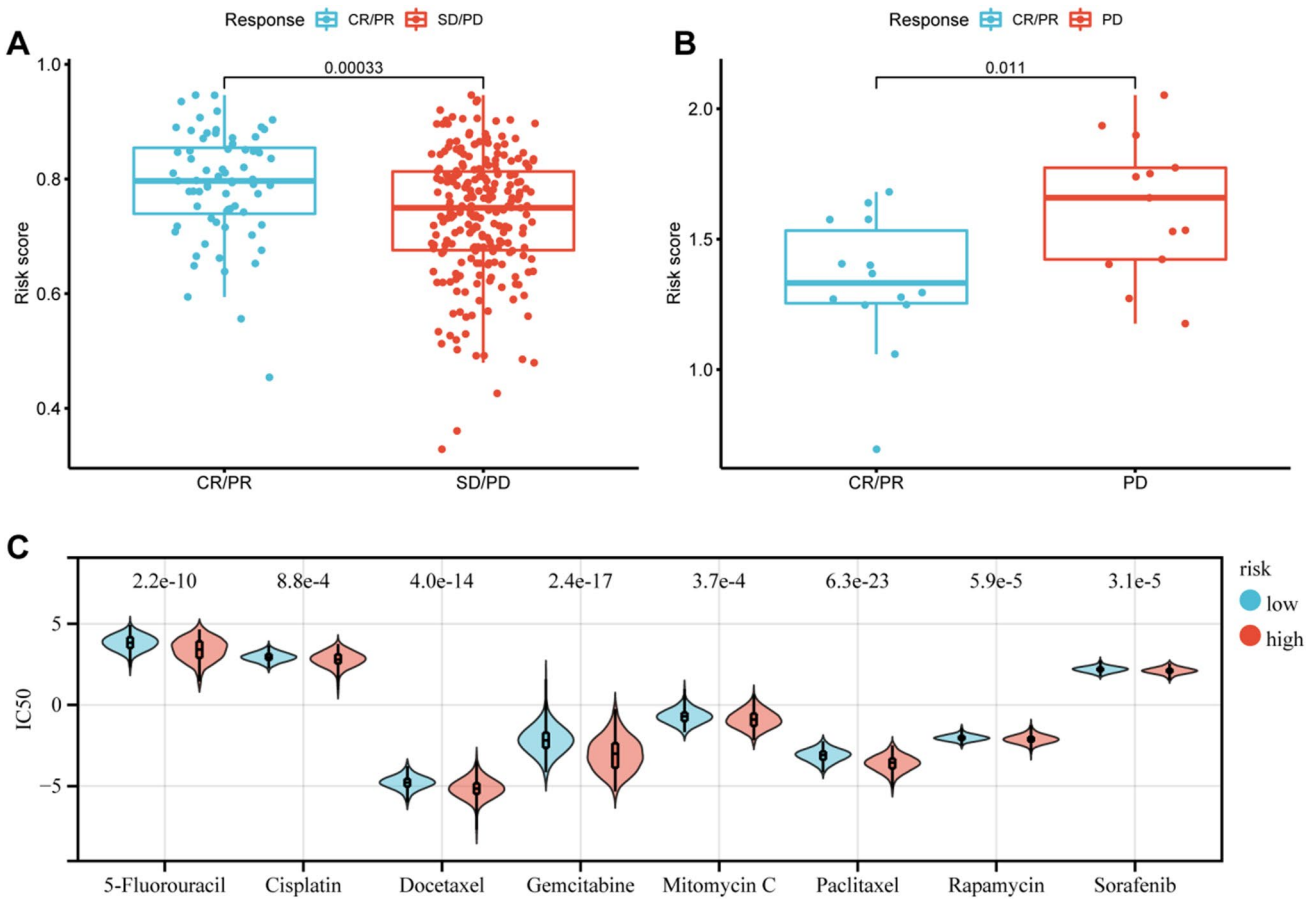

Fig. 9 The role of the KRS in predicting treatment response. (**A**) Boxplot for the KRS between anti-PD-L1 immunotherapy response and non-response groups in the IMvigor210 cohort (blue, response; red, non-response). (**B**) Boxplot for the KRS between anti-PD-1 immunotherapy response and non-response groups in the GSE78220 (blue, response; red, non-response). (**C**) Boxplot for the the half maximal inhibitory concentration (IC50) values of the chemotherapy responses between low and high KRS patients

impact on liver cancer prognosis, we conducted survival analysis on the five genes. Intriguingly, excluding PLK1, the remaining four genes demonstrated prognostic significance for liver cancer, as depicted in Fig. 10D. Based on the clinical phenotypes of each patient and the differential expression of different core genes, we performed univariate and multivariate COX regression to identify independent prognostic factors for liver cancer. Our analysis revealed that in addition to the four core genes, age, HCV infection prognosis, and bile duct invasion were independent risk factors affecting the prognosis of liver cancer patients (Supplementary Table 7). Therefore, based on our analysis of these independent factors, we constructed a nomogram graph for clinical convenience (Fig. 10E).

Discussion

HCC is a major global health concern due to its high incidence and mortality rates. Despite advancements in diagnosis and treatment, advanced and metastatic HCC still carries a poor prognosis, highlighting the urgent need for reliable prognostic biomarkers. Recent studies have identified molecular markers, including cancer-associated fibroblasts [36, 37], macrophages [38], ceRNA [39, 40], m6A-related genes [41], and hypoxia-related gene [42], that hold potential in predicting cancer prognosis and aiding in the selection of appropriate treatment strategies. These biomarkers represent promising avenues for improving clinical outcomes and deepening our understanding of HCC development and progression.

This study was designed to explore the expression patterns and prognostic significance of 538 kinase group genes in HCC tumor tissues. Through rigorous analysis, we identified 27 critical kinase-related genes and constructed two

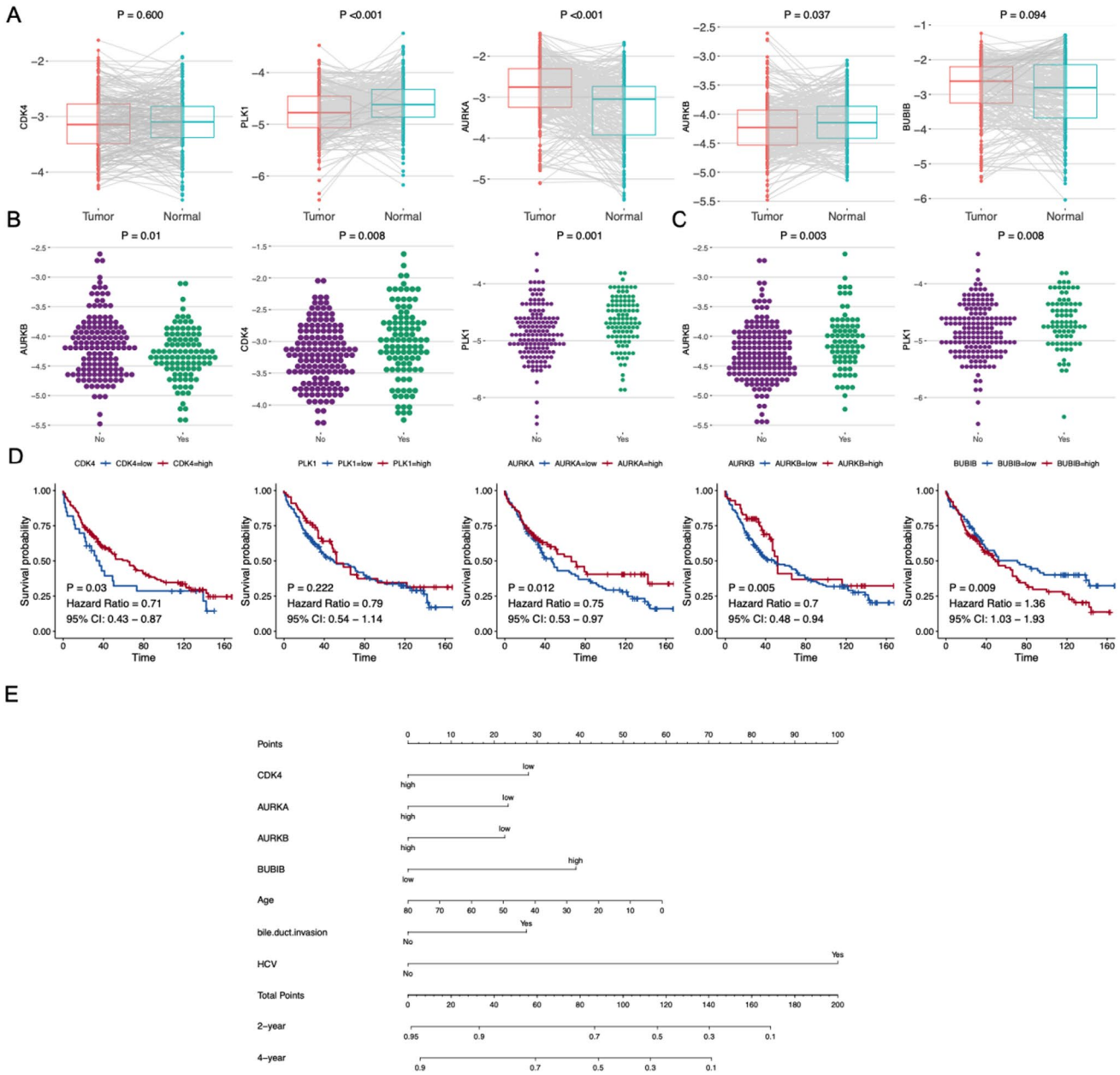

Fig. 10 Core gene expression validation. (**A**) Differential expression of five core genes in liver cancer. (**B**) Association between core genes and liver cirrhosis. (**C**) Core genes associated with tumor necrosis. (**D**) Core genes impacting prognosis of liver cancer. (**E**) nomogram for the Core gene model

distinct kinase-related subtypes within the TCGA-LIHC cohort. These subtypes demonstrated unique prognostic and immunological characteristics. Furthermore, our investigation revealed 120 DEGs associated with HCC prognosis across the subtypes. Employing univariate Cox and LASSO regression analyses, we developed a novel prognostic gene signature comprising eight kinase-related genes. The KRS derived from this signature exhibited high predictive accuracy for HCC patient prognosis and was established as an independent prognostic factor in both univariate and multivariate Cox regression analyses. Additionally, a significant correlation was observed between KRS and various forms of immune cell infiltration. Notably, KRS proved to be a reliable indicator for predicting responses to immunotherapy and chemotherapy in HCC patients. Collectively, these findings illuminate the potential clinical utility of KRS in the personalized management of liver cancer.

UAP1L1 has been reported to regulate the function of O-GlcNAc transferase, a critical factor in human hepatocellular carcinoma cell proliferation, and is associated with

breast cancer prognosis [43, 44]. Overexpression of CENPA, a fundamental protein unit of centromeres, is associated with various cancer progression types [45, 46]. TRIP13 (thyroid receptor-interacting protein 13), an AAA-ATPase family protein, is upregulated in various human cancers and promotes tumorigenesis, including hepatocellular carcinoma [47, 48]. PLGLA (plasminogen-like A) is a pseudogene of the plasminogen-encoding gene, which is preferentially expressed in the liver and has anti-tumor effects on hepatocellular carcinoma [49]. CDCA8 (human cell division cycle-associated 8), a key mitosis regulator, has been suggested as a potential prognostic biomarker and target for various cancers, such as breast, colon and hepatocellular carcinoma [50–53]. PKIB (protein kinase inhibitor-β) can interact with PKC and inhibit its activity, regulating various biological processes in cells, such as proliferation, differentiation, and apoptosis. Reports suggest that PKIB promotes the proliferation and metastasis of lung cancer, supports malignant transformation of breast cancer, promotes the infiltration of colorectal carcinoma, and is involved in the metastasis and survival of osteosarcoma [54–57]. KIF20A (Kinesin family member 20A), a member of the kinesin family, plays a critical role in cell division [58]. KIF20A is highly expressed in nearly all cancers and promotes cell proliferation, migration, and invasion, including hepatocellular carcinoma [58, 59].

Previous research has consistently demonstrated a significant link between kinases and tumor immune responses, highlighting the role of NF-kappaB-inducing kinase (NIK) as a pivotal upstream regulator of immunity [60]. In our study, hepatocellular carcinoma (HCC) samples were categorized into low- and high-Kinase-Related Score (KRS) groups, based on a kinase-focused gene signature we developed. This stratification allowed for an in-depth analysis of the differences in tumor-infiltrating immune cells and immunotherapeutic responses between these groups. Notably, the high-KRS group exhibited elevated levels of various anti-tumor immune components, including CD4+ T cells, macrophages, and B cells. Additionally, this group showed increased expression of immune checkpoint genes, MSI scores, and MHC genes. Crucially, we observed that the high KRS group was more responsive to anti-PD-L1 therapy, whereas the low KRS group showed better response to anti-PD-1 treatment. These findings suggest that KRS could serve as a valuable biomarker for tailoring therapeutic strategies and enhancing prognostic outcomes in liver cancer patients.

This study has several limitations that should be acknowledged. Firstly, the prognostic model was developed using retrospective analysis of publicly available datasets, and prospective real-world data is necessary to further validate its clinical applicability. Secondly, the predictive value of KRS in determining immunotherapy response needs to be validated in a larger sample size of HCC patients receiving immunotherapy. Moreover, further investigations are required to understand the underlying mechanisms associated with the identified kinases in HCC.

Conclusions

In summary, our study utilized 8 kinase-related genes (UAP1L1, CENPA, TRIP13, PLGLA, CDCA8, PKIB, KIF20A) to establish and validate a prognostic gene signature model called KRS, which demonstrated independent predictive power for HCC prognosis. This novel integrated model incorporating multiple genes offers a reliable tool for predicting both prognosis and therapeutic response in HCC, and provides new insights into HCC management.

Supplementary Information The online version contains supplementary material available at https://doi.org/10.1007/s10238-025-01556-8.

Acknowledgements Not applicable.

Author's contribution Conceptualization, FH and EY; methodology, YQ, XW, YL, and LS; formal analysis, software, data curation, investigation and visualization, YQ, XW, YL, LS, AG, JJ; validation, AG, JJ, LZ, and YZ; writing—original draft preparation, YQ, XW, and YL; writing—review and editing, FH and EY. All authors contributed to the article and approved the submitted version.

Funding Not applicale.

Data availability No datasets were generated or analysed during the current study.

Declarations

Conflict of interest The authors declare no competing interests.

Consent for publication The work has not been published previously, and it is not under consideration for publication elsewhere.

Ethical approval and consent to participate The research protocol was approved by the by the Ethics Committee of the Zhejiang Cancer Hospital (Ethical Approval Number: IRB-2021-234). All procedures were performed strictly in compliance with the Declaration of Helsinki 1964 or equivalent ethical principles. All patients involved in this study had given their informed consent before study.

Open Access This article is licensed under a Creative Commons Attribution-NonCommercial-NoDerivatives 4.0 International License, which permits any non-commercial use, sharing, distribution and reproduction in any medium or format, as long as you give appropriate credit to the original author(s) and the source, provide a link to the Creative Commons licence, and indicate if you modified the licensed material. You do not have permission under this licence to share adapted material derived from this article or parts of it. The images or other third party material in this article are included in the article's Creative Commons licence, unless indicated otherwise in a credit line to the material. If material is not included in the article's Creative Commons licence and your intended use is not permitted by statutory regulation or exceeds the permitted use, you will need to obtain permission directly from the copyright holder. To view a copy of this licence, visit http://creativecommons.org/licenses/by-nc-nd/4.0/.

References

1. Bray F, Laversanne M, Sung H, Ferlay J, Siegel RL, Soerjomataram I, Jemal A. Global cancer statistics 2022: GLOBOCAN estimates of incidence and mortality worldwide for 36 cancers in 185 countries. CA: A Cancer J Clin. 2024;74:229–63. https://doi.org/10.3322/caac.21834.
2. Sung H, Ferlay J, Siegel RL, Laversanne M, Soerjomataram I, Jemal A, Bray F. Global Cancer Statistics 2020: GLOBOCAN estimates of incidence and mortality worldwide for 36 cancers in 185 countries. CA Cancer J Clin. 2021;71:209–49. https://doi.org/10.3322/caac.21660.
3. Yang JD, Hainaut P, Gores GJ, Amadou A, Plymoth A, Roberts LR. A global view of hepatocellular carcinoma: trends, risk, prevention and management. Nat Rev Gastroenterol Hepatol. 2019;16:589–604. https://doi.org/10.1038/s41575-019-0186-y.
4. Yang JD, Heimbach JK. New advances in the diagnosis and management of hepatocellular carcinoma. BMJ (Clinical research ed). 2020;371: m3544. https://doi.org/10.1136/bmj.m3544.
5. Vogel A, Meyer T, Sapisochin G, Salem R, Saborowski A. Hepatocellular carcinoma. Lancet (London, England). 2022;400:1345–62. https://doi.org/10.1016/s0140-6736(22)01200-4.
6. Bray F, Ferlay J, Soerjomataram I, Siegel RL, Torre LA, Jemal A. Global cancer statistics 2018: GLOBOCAN estimates of incidence and mortality worldwide for 36 cancers in 185 countries. CA Cancer J Clin. 2018;68:394–424. https://doi.org/10.3322/caac.21492.
7. Zhang XY, Ou J, Chen JY, Li WW. Predicting early hepatocellular carcinoma recurrence after resection: a comment for moving forward. J Hepatol. 2019;70:567–8. https://doi.org/10.1016/j.jhep.2018.10.009.
8. Ardito F, Giuliani M, Perrone D, Troiano G, Lo Muzio L. The crucial role of protein phosphorylation in cell signaling and its use as targeted therapy (Review). Int J Mol Med. 2017;40:271–80. https://doi.org/10.3892/ijmm.2017.3036.
9. Manning G, Whyte DB, Martinez R, Hunter T, Sudarsanam S. The protein kinase complement of the human genome. Science. 2002;298:1912–34. https://doi.org/10.1126/science.1075762.
10. Rykx A, De Kimpe L, Mikhalap S, Vantus T, Seufferlein T, Vandenheede JR, Van Lint J. Protein kinase D: a family affair. FEBS Lett. 2003;546:81–6. https://doi.org/10.1016/s0014-5793(03)00487-3.
11. Rosenthal KJ, Gordan JD, Scott JD. Protein kinase A and local signaling in cancer. Biochem J. 2024;481:1659–77. https://doi.org/10.1042/bcj20230352.
12. Kannaiyan R, Mahadevan D. A comprehensive review of protein kinase inhibitors for cancer therapy. Expert Rev Anticancer Ther. 2018;18:1249–70. https://doi.org/10.1080/14737140.2018.1527688.
13. Bettencourt-Dias M, Giet R, Sinka R, Mazumdar A, Lock WG, Balloux F, Zafiropoulos PJ, Yamaguchi S, Winter S, Carthew RW, et al. Genome-wide survey of protein kinases required for cell cycle progression. Nature. 2004;432:980–7. https://doi.org/10.1038/nature03160.
14. Isakov N. Protein kinase C (PKC) isoforms in cancer, tumor promotion and tumor suppression. Semin Cancer Biol. 2018;48:36–52. https://doi.org/10.1016/j.semcancer.2017.04.012.
15. Bennuru S, Lustigman S, Abraham D, Nutman TB. Metabolite profiling of infection-associated metabolic markers of onchocerciasis. Mol Biochem Parasitol. 2017;215:58–69. https://doi.org/10.1016/j.molbiopara.2017.01.008.
16. Bononi A, Agnoletto C, De Marchi E, Marchi S, Patergnani S, Bonora M, Giorgi C, Missiroli S, Poletti F, Rimessi A, et al. Protein kinases and phosphatases in the control of cell fate. Enzyme Res. 2011;2011: 329098. https://doi.org/10.4061/2011/329098.
17. Gross S, Rahal R, Stransky N, Lengauer C, Hoeflich KP. Targeting cancer with kinase inhibitors. J Clin Invest. 2015;125:1780–9. https://doi.org/10.1172/JCI76094.
18. Fleuren ED, Zhang L, Wu J, Daly RJ. The kinome "at large" in cancer. Nat Rev Cancer. 2016;16:83–98. https://doi.org/10.1038/nrc.2015.18.
19. Schram AM, Chang MT, Jonsson P, Drilon A. Fusions in solid tumours: diagnostic strategies, targeted therapy, and acquired resistance. Nat Rev Clin Oncol. 2017;14:735–48. https://doi.org/10.1038/nrclinonc.2017.127.
20. Du Z, Lovly CM. Mechanisms of receptor tyrosine kinase activation in cancer. Mol Cancer. 2018;17:58. https://doi.org/10.1186/s12943-018-0782-4.
21. Yesilkanal AE, Johnson GL, Ramos AF, Rosner MR. New strategies for targeting kinase networks in cancer. J Biol Chem. 2021;297: 101128. https://doi.org/10.1016/j.jbc.2021.101128.
22. Roskoski R Jr. Properties of FDA-approved small molecule protein kinase inhibitors: a 2024 update. Pharmacol Res. 2024;200:107059. https://doi.org/10.1016/j.phrs.2024.107059.
23. Wang C, Vegna S, Jin H, Benedict B, Lieftink C, Ramirez C, de Oliveira RL, Morris B, Gadiot J, Wang W, et al. Inducing and exploiting vulnerabilities for the treatment of liver cancer. Nature. 2019;574:268–72. https://doi.org/10.1038/s41586-019-1607-3.
24. Kudo M, Finn RS, Qin S, Han KH, Ikeda K, Piscaglia F, Baron A, Park JW, Han G, Jassem J, et al. Lenvatinib versus sorafenib in first-line treatment of patients with unresectable hepatocellular carcinoma: a randomised phase 3 non-inferiority trial. Lancet. 2018;391:1163–73. https://doi.org/10.1016/S0140-6736(18)30207-1.
25. Wei S, Zhang J, Shi R, Yu Z, Chen X, Wang H. Identification of an integrated kinase-related prognostic gene signature associated with tumor immune microenvironment in human uterine corpus endometrial carcinoma. Front Oncol. 2022;12: 944000. https://doi.org/10.3389/fonc.2022.944000.
26. Ritchie ME, Phipson B, Wu D, Hu Y, Law CW, Shi W, Smyth GK. limma powers differential expression analyses for RNA-sequencing and microarray studies. Nucleic Acids Res. 2015;43:e47. https://doi.org/10.1093/nar/gkv007.
27. Zhou Y, Zhou B, Pache L, Chang M, Khodabakhshi AH, Tanaseichuk O, Benner C, Chanda SK. Metascape provides a biologist-oriented resource for the analysis of systems-level datasets. Nat Commun. 2019;10:1523. https://doi.org/10.1038/s41467-019-09234-6.
28. Wilkerson MD, Hayes DN. ConsensusClusterPlus: a class discovery tool with confidence assessments and item tracking. Bioinformatics. 2010;26:1572–3. https://doi.org/10.1093/bioinformatics/btq170.
29. Lu SY, Hua J, Liu J, Wei MY, Liang C, Meng QC, Zhang B, Yu XJ, Wang W, Xu J. Construction of a paclitaxel-related competitive endogenous RNA network and identification of a potential regulatory axis in pancreatic cancer. Transl Oncol. 2022;20:101419. https://doi.org/10.1016/j.tranon.2022.101419.
30. Yoshihara K, Shahmoradgoli M, Martínez E, Vegesna R, Kim H, Torres-Garcia W, Treviño V, Shen H, Laird PW, Levine DA, et al. Inferring tumour purity and stromal and immune cell admixture from expression data. Nat Commun. 2013;4:2612. https://doi.org/10.1038/ncomms3612.
31. Wang H, Lu X, Chen J. Construction and experimental validation of an acetylation-related gene signature to evaluate the recurrence and immunotherapeutic response in early-stage lung adenocarcinoma. BMC Med Genomics. 2022;15:254. https://doi.org/10.1186/s12920-022-01413-7.
32. Shen W, Song Z, Zhong X, Huang M, Shen D, Gao P, Qian X, Wang M, He X, Wang T, et al. Sangerbox: a comprehensive, interaction-friendly clinical bioinformatics analysis platform. iMeta. 2022;1:e36. https://doi.org/10.1002/imt2.36.

33. Yu G, Wang LG, Han Y, He QY. clusterProfiler: an R package for comparing biological themes among gene clusters. OMICS. 2012;16:284–7. https://doi.org/10.1089/omi.2011.0118.
34. Geeleher P, Cox N, Huang RS. pRRophetic: an R package for prediction of clinical chemotherapeutic response from tumor gene expression levels. PLoS ONE. 2014;9: e107468. https://doi.org/10.1371/journal.pone.0107468.
35. Yang W, Soares J, Greninger P, Edelman EJ, Lightfoot H, Forbes S, Bindal N, Beare D, Smith JA, Thompson IR, et al. Genomics of Drug Sensitivity in Cancer (GDSC): a resource for therapeutic biomarker discovery in cancer cells. Nucleic Acids Res. 2013;41:D955–61. https://doi.org/10.1093/nar/gks1111.
36. Gui Z, Ye Y, Li Y, Ren Z, Wei N, Liu L, Wang H, Zhang M. Construction of a novel cancer-associated fibroblast-related signature to predict clinical outcome and immune response in cervical cancer. Transl Oncol. 2024;46: 102001. https://doi.org/10.1016/j.tranon.2024.102001.
37. Ye Y, Zhang S, Jiang Y, Huang Y, Wang G, Zhang M, Gui Z, Wu Y, Bian G, Li P, et al. Identification of a cancer associated fibroblasts-related index to predict prognosis and immune landscape in ovarian cancer. Sci Rep. 2023;13:21565. https://doi.org/10.1038/s41598-023-48653-w.
38. Yang Z, Zi Q, Xu K, Wang C, Chi Q. Development of a macrophages-related 4-gene signature and nomogram for the overall survival prediction of hepatocellular carcinoma based on WGCNA and LASSO algorithm. Int Immunopharmacol. 2021;90: 107238. https://doi.org/10.1016/j.intimp.2020.107238.
39. Long J, Bai Y, Yang X, Lin J, Yang X, Wang D, He L, Zheng Y, Zhao H. Construction and comprehensive analysis of a ceRNA network to reveal potential prognostic biomarkers for hepatocellular carcinoma. Cancer Cell Int. 2019;19:90. https://doi.org/10.1186/s12935-019-0817-y.
40. Zhang L, Tao H, Li J, Zhang E, Liang H, Zhang B. Comprehensive analysis of the competing endogenous circRNA-lncRNA-miRNA-mRNA network and identification of a novel potential biomarker for hepatocellular carcinoma. Aging (Albany NY). 2021;13:15990–6008. https://doi.org/10.18632/aging.203056.
41. Liu J, Sun G, Pan S, Qin M, Ouyang R, Li Z, Huang J. The Cancer Genome Atlas (TCGA) based m(6)A methylation-related genes predict prognosis in hepatocellular carcinoma. Bioengineered. 2020;11:759–68. https://doi.org/10.1080/21655979.2020.1787764.
42. Zhang B, Tang B, Gao J, Li J, Kong L, Qin L. A hypoxia-related signature for clinically predicting diagnosis, prognosis and immune microenvironment of hepatocellular carcinoma patients. J Transl Med. 2020;18:342. https://doi.org/10.1186/s12967-020-02492-9.
43. Hill VK, Ricketts C, Bieche I, Vacher S, Gentle D, Lewis C, Maher ER, Latif F. Genome-wide DNA methylation profiling of CpG islands in breast cancer identifies novel genes associated with tumorigenicity. Cancer Res. 2011;71:2988–99. https://doi.org/10.1158/0008-5472.CAN-10-4026.
44. Lai CY, Liu H, Tin KX, Huang Y, Yeh KH, Peng HW, Chen HD, He JY, Chiang YJ, Liu CS, et al. Identification of UAP1L1 as a critical factor for protein O-GlcNAcylation and cell proliferation in human hepatoma cells. Oncogene. 2019;38:317–31. https://doi.org/10.1038/s41388-018-0442-6.
45. Athwal RK, Walkiewicz MP, Baek S, Fu S, Bui M, Camps J, Ried T, Sung MH, Dalal Y. CENP-A nucleosomes localize to transcription factor hotspots and subtelomeric sites in human cancer cells. Epigen Chromatin. 2015;8:2. https://doi.org/10.1186/1756-8935-8-2.
46. Renaud-Pageot C, Quivy JP, Lochhead M, Almouzni G. CENP-a regulation and cancer. Front Cell Dev Biol. 2022;10: 907120. https://doi.org/10.3389/fcell.2022.907120.
47. Wang Y, Huang J, Li B, Xue H, Tricot G, Hu L, Xu Z, Sun X, Chang S, Gao L, et al. A small-molecule inhibitor targeting TRIP13 suppresses multiple myeloma progression. Cancer Res. 2020;80:536–48. https://doi.org/10.1158/0008-5472.CAN-18-3987.
48. Zhu MX, Wei CY, Zhang PF, Gao DM, Chen J, Zhao Y, Dong SS, Liu BB. Elevated TRIP13 drives the AKT/mTOR pathway to induce the progression of hepatocellular carcinoma via interacting with ACTN4. J Exp Clin Cancer Res. 2019;38:409. https://doi.org/10.1186/s13046-019-1401-y.
49. Bao L, Li P, Zhao H, Chen L, Wang Y, Liang S, Liu J. Pseudogene PLGLA exerts anti-tumor effects on hepatocellular carcinoma through modulating miR-324-3p/GLYATL1 axis. Dig Liver Dis. 2022;54:918–26. https://doi.org/10.1016/j.dld.2021.10.003.
50. Cui XH, Peng QJ, Li RZ, Lyu XJ, Zhu CF, Qin XH. Cell division cycle associated 8: a novel diagnostic and prognostic biomarker for hepatocellular carcinoma. J Cell Mol Med. 2021;25:11097–112. https://doi.org/10.1111/jcmm.17032.
51. Shuai Y, Fan E, Zhong Q, Chen Q, Feng G, Gou X, Zhang G. CDCA8 as an independent predictor for a poor prognosis in liver cancer. Cancer Cell Int. 2021;21:159. https://doi.org/10.1186/s12935-021-01850-x.
52. Wang Y, Zhao Z, Bao X, Fang Y, Ni P, Chen Q, Zhang W, Deng A. Borealin/Dasra B is overexpressed in colorectal cancers and contributes to proliferation of cancer cells. Med Oncol. 2014;31:248. https://doi.org/10.1007/s12032-014-0248-5.
53. Yu D, Shi L, Bu Y, Li W. Cell division cycle associated 8 is a key regulator of tamoxifen resistance in breast cancer. J Breast Cancer. 2019;22:237–47. https://doi.org/10.4048/jbc.2019.22.e29.
54. Dou P, Zhang D, Cheng Z, Zhou G, Zhang L. PKIB promotes cell proliferation and the invasion-metastasis cascade through the PI3K/Akt pathway in NSCLC cells. Exp Biol Med (Maywood). 2016;241:1911–8. https://doi.org/10.1177/1535370216655908.
55. Wan R, Yang G, Liu Q, Fu X, Liu Z, Miao H, Liu H, Huang W. PKIB involved in the metastasis and survival of osteosarcoma. Front Oncol. 2022;12: 965838. https://doi.org/10.3389/fonc.2022.965838.
56. Wang HW, Duan ZJ, Hu SS, Wang S. Expression of cAMP-dependent protein kinase inhibitor beta in colorectal carcinoma and its clinical significance. Nan Fang Yi Ke Da Xue Xue Bao. 2017;37:744–9. https://doi.org/10.3969/j.issn.1673-4254.2017.06.05.
57. Zhang JB, Song W, Wang YY, Liu MG, Sun MM, Liu H. Study on correlation between PKIB and pAkt expression in breast cancer tissues. Eur Rev Med Pharmacol Sci. 2017;21:1264–9.
58. Jin Z, Peng F, Zhang C, Tao S, Xu D, Zhu Z. Expression, regulating mechanism and therapeutic target of KIF20A in multiple cancer. Heliyon. 2023;9: e13195. https://doi.org/10.1016/j.heliyon.2023.e13195.
59. Shi C, Huang D, Lu N, Chen D, Zhang M, Yan Y, Deng L, Lu Q, Lu H, Luo S. Aberrantly activated Gli2-KIF20A axis is crucial for growth of hepatocellular carcinoma and predicts poor prognosis. Oncotarget. 2016;7:26206–19. https://doi.org/10.18632/oncotarget.8441.
60. Pflug KM, Sitcheran R. Targeting NF-kappaB-Inducing Kinase (NIK) in immunity, inflammation, and cancer. Int J Mol Sci. 2020. https://doi.org/10.3390/ijms21228470.

Publisher's Note Springer Nature remains neutral with regard to jurisdictional claims in published maps and institutional affiliations.